Intervention Serology and Interaction Substitution: Exploring the Role of 'Immune Shielding' in Reducing COVID-19 Epidemic Spread
Supplementary Information

Joshua S. Weitz,[1,2,3,*] Stephen J. Beckett,[1] Ashley R. Coenen,[2] David Demory,[1] Marian Dominguez-Mirazo,[4,1] Jonathan Dushoff,[5,6] Chung-Yin Leung,[1,2] Guanlin Li,[4,2] Andreea Magalie,[4,1] Sang Woo Park,[7] Rogelio Rodriguez-Gonzalez,[4,1] Shashwat Shivam,[8] and Conan Zhao[4,1]

[1] *School of Biological Sciences, Georgia Institute of Technology, Atlanta, GA, USA*
[2] *School of Physics, Georgia Institute of Technology, Atlanta, GA, USA*
[3] *Center for Microbial Dynamics and Infection, Georgia Institute of Technology, Atlanta, GA, USA*
[4] *Interdisciplinary Graduate Program in Quantitative Biosciences, Georgia Institute of Technology, Atlanta, GA, USA*
[5] *Department of Biology, McMaster University, Hamilton, ON, Canada*
[6] *DeGroote Institute for Infectious Disease Research, McMaster University, Hamilton, ON, Canada*
[7] *Department of Ecology and Evolutionary Biology, Princeton University, Princeton, NJ, USA*
[8] *School of Electrical and Computer Engineering, Georgia Institute of Technology, Atlanta, GA, USA*

(Dated: March 31, 2020)

Contents

*Electronic address: jsweitz@gatech.edu; URL: http://ecotheory.biology.gatech.edu

I. MODEL AND PARAMETERS

Assumptions for Age-Structured Model

We present the age-structured epidemiological model discussed in the main text. Consider a population of susceptible S, exposed E, infectious asymptomatic I_{asym}, infectious symptomatic I_{sym}, and recovered R who are free to move, without restrictions in a 'business as usual' scenario. A subset of symptomatic cases will require hospital care, which we further divide into subacute I_{hsub}, and critical/acute (i.e., requiring ICU intervention) I_{hcrit} cases. Vital dynamics (births and other causes of death) are ignored for simplicity. The model is visually represented in Fig S1 and the system of nonlinear differential equations governing this age-structured epidemiological model are shown below:

$$
\begin{aligned}
\frac{dS(a)}{dt} &= -\overbrace{\frac{\beta_s S(a) I_{sym,tot}}{N_{tot}+\alpha R_{Shields}}}^{symptomatic\ contact} - \overbrace{\frac{\beta_{asym} S(a) I_{asym,tot}}{N_{tot}+\alpha R_{Shields}}}^{asymptomatic\ contact} \\
\frac{dE(a)}{dt} &= \overbrace{\frac{\beta_{sym} S(a) I_{sym,tot}}{N_{tot}+\alpha R_{Shields}}}^{symptomatic\ contact} + \overbrace{\frac{\beta_{asym} S(a) I_{asym,tot}}{N_{tot}+\alpha R_{Shields}}}^{asymptomatic\ contact} - \overbrace{\gamma_e E(a)}^{onset\ of\ infectiousness} \\
\frac{dI_{asym}(a)}{dt} &= \overbrace{p(a)\gamma_e E(a)}^{asymptomatic\ onset} - \overbrace{\gamma_a I_{asym}(a)}^{recovery} \\
\frac{dI_{sym}(a)}{dt} &= \overbrace{(1-p(a))\gamma_e E(a)}^{symptomatic\ onset} - \overbrace{\gamma_s I_{sym}(a)}^{transfer\ from\ I_{sym}} \\
\frac{dI_{hsub}(a)}{dt} &= \overbrace{h(a)(1-\xi(a))\gamma_s I_{sym}(a)}^{subcritical\ cases} - \overbrace{\gamma_h I_{hsub}(a)}^{transfer\ from\ I_{hsub}} \\
\frac{dI_{hcrit}(a)}{dt} &= \overbrace{h(a)\xi(a)\gamma_s I_{sym}(a)}^{critical\ (ICU)\ cases} - \overbrace{\gamma_h I_{hcrit}(a)}^{transfer\ from\ I_{hcrit}} \\
\frac{dR(a)}{dt} &= \overbrace{\gamma_a I_{asym}(a)}^{recovery\ from\ I_{asym}} - \overbrace{(1-h(a))\gamma_s I_{sym}(a)}^{recovery\ from\ I_{sym}} - \overbrace{\gamma_h I_{hsub}(a)}^{recovery\ from\ I_{hsub}} - \overbrace{(1-\mu)\gamma_h I_{hcrit}(a)}^{recovery\ from\ I_{hcrit}} \\
\frac{dD(a)}{dt} &= \overbrace{\mu\gamma_h I_{hcrit}(a)}^{mortality},
\end{aligned}
$$

where $I_{sym,tot}$ are the total number (across all age classes) of symptomatic infectious individuals, $I_{asym,tot}$ are the total number of asymptomatic infectious individuals, N_{tot} is the total number of alive individuals (not in the D state), and $R_{Shields}$ are the number of recovered individuals who could serve as serological shields - which we define as those of ages between 20 and 59. The assumed model parameters used in the baseline models are shown in tables S1 and S2.

Parameter	Meaning	Value
β_a	Asymptomatic transmission	0.3/day
β_s	Symptomatic transmission	0.6/day
$1/\gamma_e$	Mean exposed period	4 days
$1/\gamma_a$	Mean asymptomatic period	4 (low) and 6 (high) days
$1/\gamma_s$	Mean symptomatic period	4 (low) and 6 (high) days
$1/\gamma_h$	Mean hospital period	10 days
$\mathcal{R}_0$	Basic reproduction number	1.57 (low) and 2.33 (high)

TABLE S1: Epidemiological characteristics.

Age	Frac. of Population f	Frac. Asymptomatic p	Hospital Frac. h	ICU (given hospitalization) Frac. ξ
0-9	0.12	0.95	0.001	0.05
10-19	0.14	0.95	0.003	0.05
20-29	0.14	0.9	0.012	0.05
30-39	0.13	0.8	0.032	0.05
40-49	0.13	0.7	0.049	0.063
50-59	0.13	0.6	0.102	0.122
60-69	0.10	0.4	0.166	0.274
70-79	0.06	0.2	0.243	0.432
80-89	0.04	0.2	0.273	0.709
90-99	0.01	0.2	0.273	0.709

TABLE S2: Age-stratified risk for COVID-19. Of note, the model assumes that 50% of ICU cases die. Parameters in line with [1].

Varying the intensity of the outbreak $\mathcal{R}_0$

Based on the parameters in tables S1 and S2 $\mathcal{R}_0$ is calculated as a weighted average between the symptomatic and asymptomatic reproduction numbers R_{asym}, respectively R_{sym}:

$$R_0 = pR_{asym} + (1-p)R_{sym}. \tag{1}$$

These can be further expanded based on age groups to obtain:

$$R_0 = \sum_{a \in \text{Age Groups}} p(a) \cdot f(a) \cdot R_{asym}(a) + (1-p(a)) \cdot f(a) \cdot R_{sym}(a). \tag{2}$$

which yields a basic reproduction number of about 1.57 in the low scenario and 2.33 in the high scenario.

Initial conditions in the extended model

The baseline model assumes a population of 10,000,000 with age demographics as given in Table S2 unless stated otherwise. An initial outbreak is seeded in this population given one exposed individual in the 20-29 age class. The simulation is run forward until 10,000 people have been exposed to the virus (i.e. 10,000 people are no longer in the susceptible states) - we use this time point (which we denote time 0 in our simulations) as the time at which intervention policies might be applied. At this point, once 10,000 people have already been exposed we simulate the dynamics forward either with, or without the interventions, described in the main text and below.

II. INTERACTION SUBSTITUTION AND DEMOGRAPHY

Demography has potential impacts on the spread and consequences of coronavirus and on the efficacy of intervention strategies. We evaluated the baseline model and shielding scenarios $\alpha = 2$ and $\alpha = 20$ given the age structure for the United States, i.e., including 50 states, Washington D.C., and Puerto Rico. The states include significant variation in the fraction of population over 60, ranging from less than 16% (Utah) to above 28% (Maine). We observe a demographic dependence on efficacy of shielding to both per capita cumulative deaths and per capita peak ICU demand, linked to the fraction of the population that is 60 and above. The relationship is linear under both the low and high $\mathcal{R}_0$ scenarios (see Figures S2 and S3). Outcomes are better when the population has relatively more younger individuals (given that age stratified risk will favor improved outcomes for those who are infected). However, notably, shielding reduces the difference in outcomes, e.g., whereas the cumulative deaths for Utah are 440 (400) less per 100,000 than Maine in the baseline case they are only 210 (120) less per 100,000 than Maine in the $\alpha = 20$ shielding case for the high (low) $\mathcal{R}_0$ scenarios. Hence, demographic distributions that are relatively older will favor deployment of shields (in a relative sense). We note that although we have treated state level demographics uniformly, this result also points toward urban areas with right-shifted age distributions as potential targets for intervention - and potential consequences for deployment of shields in other countries with right-shifted demographics (e.g., Italy).

III. VARIATION WITH ASYMPTOMATIC CASES

We investigate the impact of asymptomatic transmission on the efficacy of immune shielding as an intervention. First, we fixed the intrinsic asymptomatic fraction p from 0.5 to 0.95 for scenarios corresponding to $\alpha = 0, 2$ and 20 (SI Fig S4). Irrespective of the shielding preference α increases in p reduces total deaths and ICU cases by $\approx 90\%$ when R_0 is constant and more than 90% when R_0 is a function of p, given variation from $p = 0.5$ to $p = 0.95$. We observed that the impact of immune shielding is higher at low p. Second, we consider the effects of age-dependent variation in the intrinsic asymptomatic fraction, $p(a)$, by fixing the average p at 0.5, 0.75 and 0.9, given observations of increasing risk based on clinical outcome data from Wuhan, China [2] (SI Fig S5). The impact of immune shielding is robust to observed age-specific variation p, i.e., leading to significant decreases of projected deaths and ICU cases (SI Fig. S6).

IV. IMPACTS OF WANING IMMUNITY

We extended the core model to account for potential impacts of waning immunity by including explicit state-structured shield compartments consisting of newly recruited recovered individuals (H_1) and late stage recovered individuals that can revert to become susceptible (H_2). In effect, the immunity duration was assumed to be gamma distributed, after which recovered individuals become susceptible. This is a conservative assumption, given that individual who lose immunity are likely to have less severe illness if re-infected (but could still pass on an infection to immunological naive individuals).

Figure S7 shows the outbreak dynamics for the high and low R_0 scenarios with an average immunity duration of 2 months. Immune shielding can still significantly reduce the number of deaths and the peak number of ICU beds needed for both scenarios, especially for the strong shielding case ($\alpha = 20$). In Fig. S8, we systematically explore how the cumulative deaths, maximum ICU beds needed, and total number of cases depend on the immunity duration. The results show that the efficacy of immune shielding is robust to the duration of immunity, insofar as the duration of immunity persists on the order of multiple months (and not multiple weeks).

V. OPTIMISED AGE-DEPENDENT IMMUNE SHIELDING DEPLOYMENT

In the previous sections, we assumed that shields (recovered individuals aged 20-59) were deployed such that they interact with people of all ages equally. In other words, all the susceptible individuals (across ages) have an infection rate that scales with $I_{tot}/(N_{tot}+\alpha R_{shields})$ such that the shields are uniformly interacting with all ages. In this section, we explore the outcome of having the shields act in positions where they could be more or less-likely to interact with different age groups, *i.e.,* using the same effort as in the core model, then taking the $\alpha R_{shields}$ of effort but distributing it non-uniformly across ages. To explore the 'optimised' distributions of the shields effort, we introduce non-uniform shield interactions in the model. To do so, we modify the equations of $S(a)$ and $E(a)$ in the core model as follows:

$$\begin{aligned}\frac{dS(a)}{dt} &= -\beta_a \frac{S(a)I_{asym,tot}}{N_{tot} + \alpha R_{shields}(\theta_a/f_a)} - \beta_s \frac{S(a)I_{sym,tot}}{N_{tot} + \alpha R_{shields}(\theta_a/f_a)} \\ \frac{dE(a)}{dt} &= \beta_a \frac{S(a)I_{asym,tot}}{N_{tot} + \alpha R_{shields}(\theta_a/f_a)} + \beta_s \frac{S(a)I_{sym,tot}}{N_{tot} + \alpha R_{shields}(\theta_a/f_a)} - \gamma_e E(a),\end{aligned} \tag{3}$$

where f_a is the fraction of the population of age a (f_a-s are fixed parameters) and θ_a is the distributed shielding fraction of the sub-population class of age a, i.e. how we distribute the shields to interact across different age classes. θ_a are the optimization variables. In addition, we define the ratio θ_a/f_a as the age-dependent shielding concentration. When $f_a/\theta_a = 1$ for all ages a, the uniform shields interactions case is recovered i.e. we recover the core model. We note that $\sum_a \theta_a = 1$ such that the effort is the same as in the core model, but allowing for asymmetric distribution across ages. For example, if 25% percent of the population belongs to class a and gets all the shields protection, then $f_a = 0.25$ and $\theta_a = 1$, this implies $\theta_a/f_a = 4$, i.e. a 4-fold boosted protection for that particular class.

The optimization objective here is to minimize total deaths $D_{tot}(t_f)$, where t_f is the final time of the simulation – 1 year after shielding begins, while keeping ICU beds less than the maximum carrying capacity B at every time instant. We seek to find the optimum distribution for deploying the effort of the serological shields. The non-uniform shielding fraction can be represent by a vector $\Theta = [\theta_1, \ ..., \ \theta_{10}]$, and we aim to solve the following minimization problem:

$$\min \mathcal{J}(\Theta) = \int_{t_0}^{t_f} \overbrace{W_i \times d(I_{hcri}^{tot}(t))}^{\text{barrier function (constraint)}} \; dt \; + \; \overbrace{W_d \times D_{tot}(t_f)}^{\text{costs of deaths}}, \tag{4}$$

$$\text{subject to } \sum_{a=1}^{10} \theta_a = 1 \; , \; \theta_a \geq 0 \quad \forall \; a = 1, \; 2, \; ..., \; 10; \tag{5}$$

where W_i are W_d are weight regulators. The barrier function d is chosen such that it increases the cost dramatically as the number of ICU beds in use approach the capacity B of the system, to prevent overloading the healthcare system. To satisfy this property, we pick $d(x) = \log\left(\frac{1}{B-x}\right)$. The barrier function goes to infinity as x approaches B from the left. Here, we consider the maximum capacity B as a 'strict' (or 'hard') constraint and any distributed shielding fraction Θ that leads to the ICU beds exceeding B is not considered a feasible shielding deployment. Given the simulation results shown in main text, we set B as 200 ICU beds per 100,000 for the high scenario case and $B = 80$ ICU beds per 100,000 people for the low scenario case. Note that at this point we are trying to see if we can improve the effectiveness of serological shields, by deploying them unevenly across a population, rather than to keep the maximum number of ICU patients below a realistic capacity (actual ICU capacity may be lower than the values chosen here [1]). Moreover, the barrier function in the cost function is negative if $I_{hcri}(t) < B - 1$, which is a 'reward' if occupancy of the ICU beds is low. In practice, we set W_i to be arbitrarily small since it serves much like a constraint, e.g., $W_i = 10^{-7}$. We let $W_d = 1$ as minimizing deaths is the primary goal. The optimization problem (eq. 4) is solved via a *genetic algorithm* [3] using `matlab's` built-in optimization function `ga`, with the maximum generation number (set to 30) serving as the stopping criterion [4].

Figures S9, S10 shows that an improved way of distributing shielding effort is: low, but non-zero, shielding of young; with increasing effort for elderly members of the population (see Fig S11). Using the optimized shielding deployment, the reduction in deaths ($D_{tot}(t_f)$) is significant. The results suggest that we should try to preferentially shield those who are most at risk.

VI. FIGURES

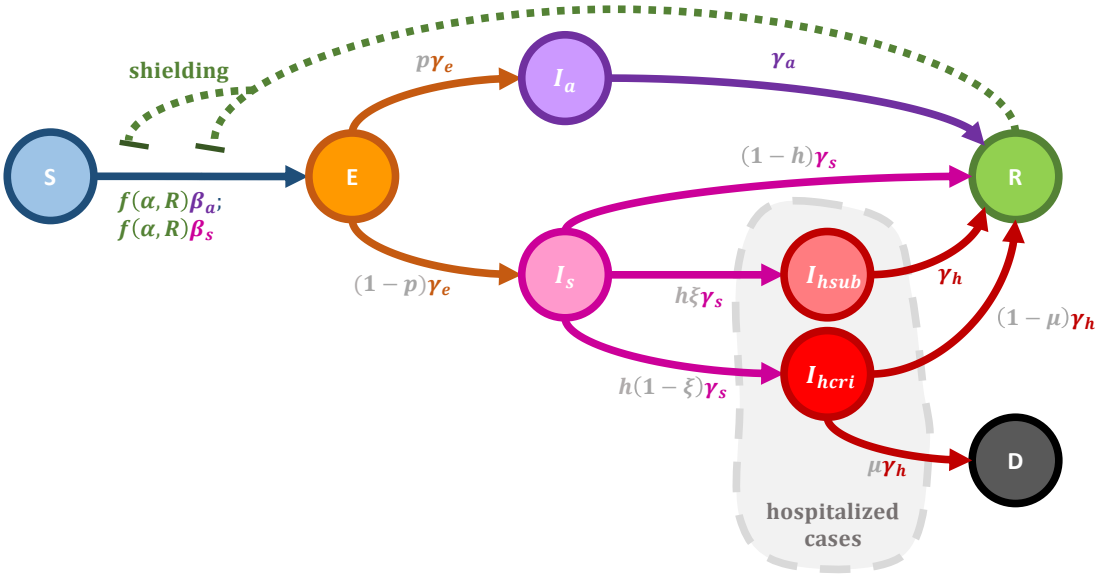

FIG. S1: Model schematic. We consider a population susceptible individuals (S), interacting with infected (I_{sym}, I_{asym}) and recovered (R) individuals. Interactions between susceptible and infectious individuals lead to new exposed cases (E). Exposed individuals undergo a period of latency before disease onset, which are symptomatic (I_{sym}) or asymptomatic (I_{asym}). A subset of symptomatic individuals require hospitalization (I_h) which we further categorize as acute/subcritical (I_{hsub}) and critical (I_{hcri}) cases, the latter of which can be fatal. Individuals who recover can then mitigate the rate of new exposure cases by interaction substitution - what we denote as *immune shielding* - by modulating the rate of susceptible-infectious interactions by ω_{asym} and ω_{sym} respectively, where $\omega_{asym} = \frac{S(a)I_{asym,tot}}{N_{tot}+\alpha R_{shields}}$. Here, the *tot* subscript denotes the total number of cases across all ages, i.e. $I_{sym,tot} = \sum_a I_{sym}(a)$.

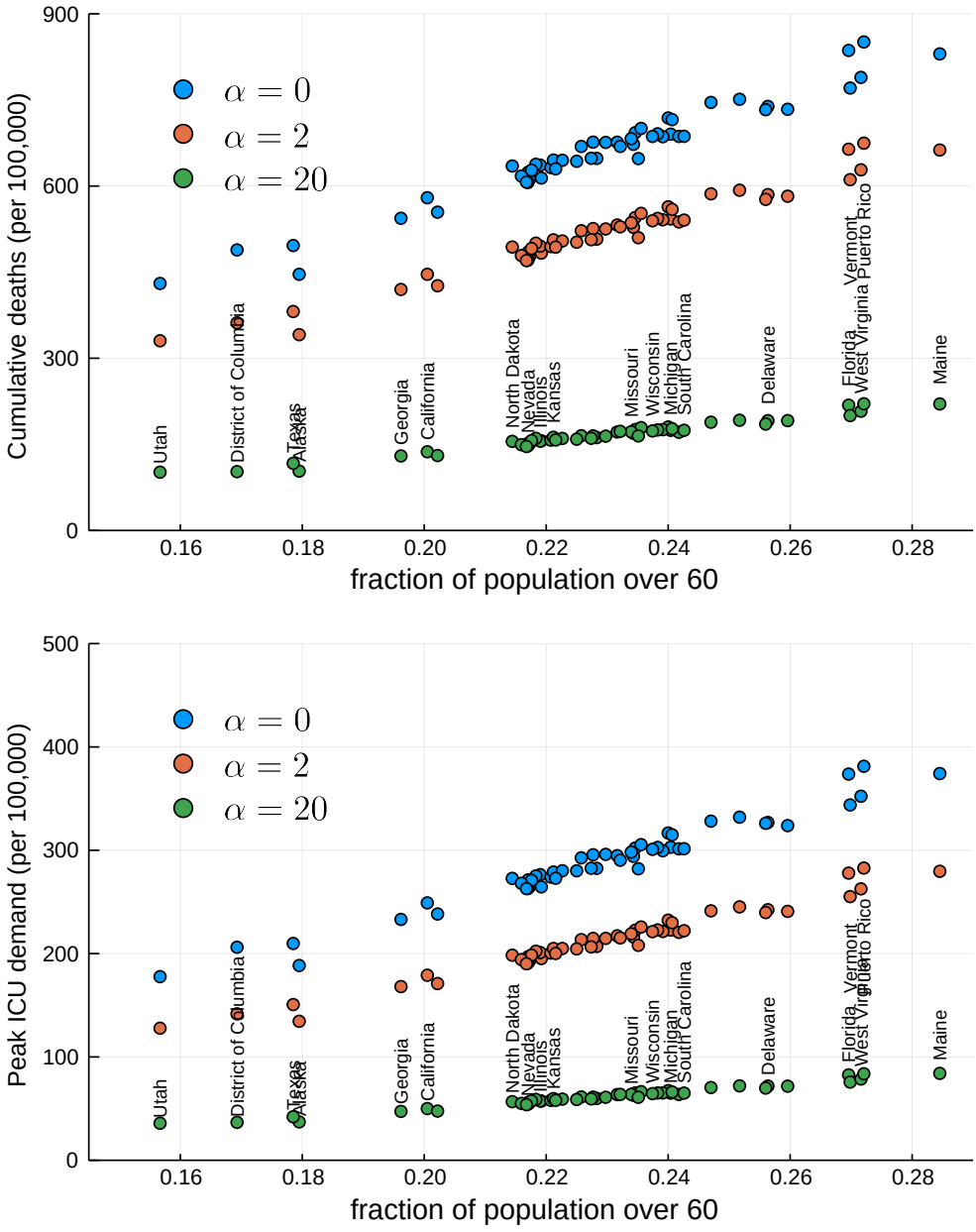

FIG. S2: Impact of demography on the intervention benefits of immune shielding in a low $\mathcal{R}_0$ scenario. States are ordered by fraction of population above 60 (x-axis) with the baseline, low and high shielding scenarios shown; labels of some but not all states are shown for clarity.

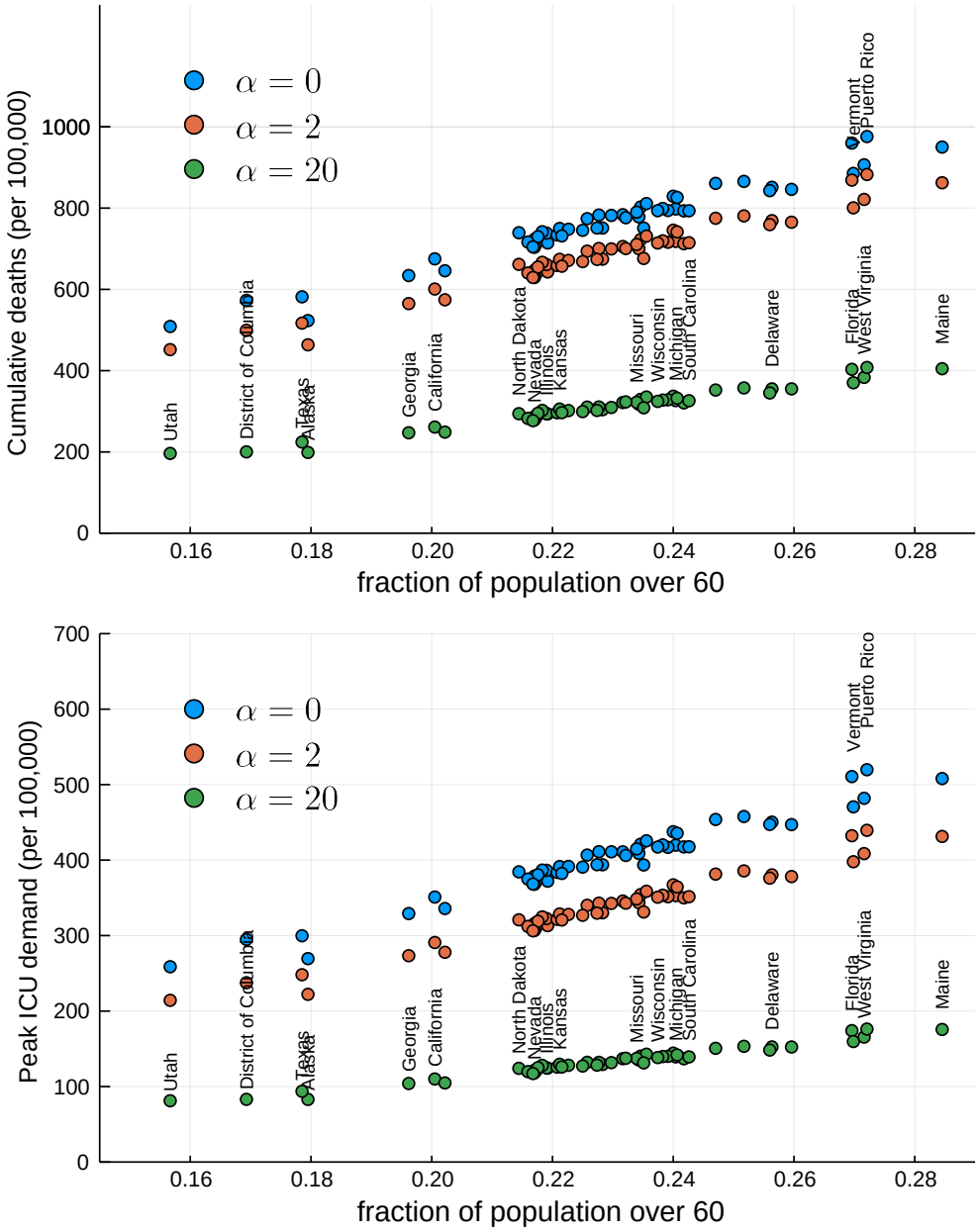

FIG. S3: Impact of demography on the intervention benefits of immune shielding in a high $\mathcal{R}_0$ scenario. States are ordered by fraction of population above 60 (x-axis) with the baseline, low and high shielding scenarios shown; labels of some but not all states are shown for clarity.

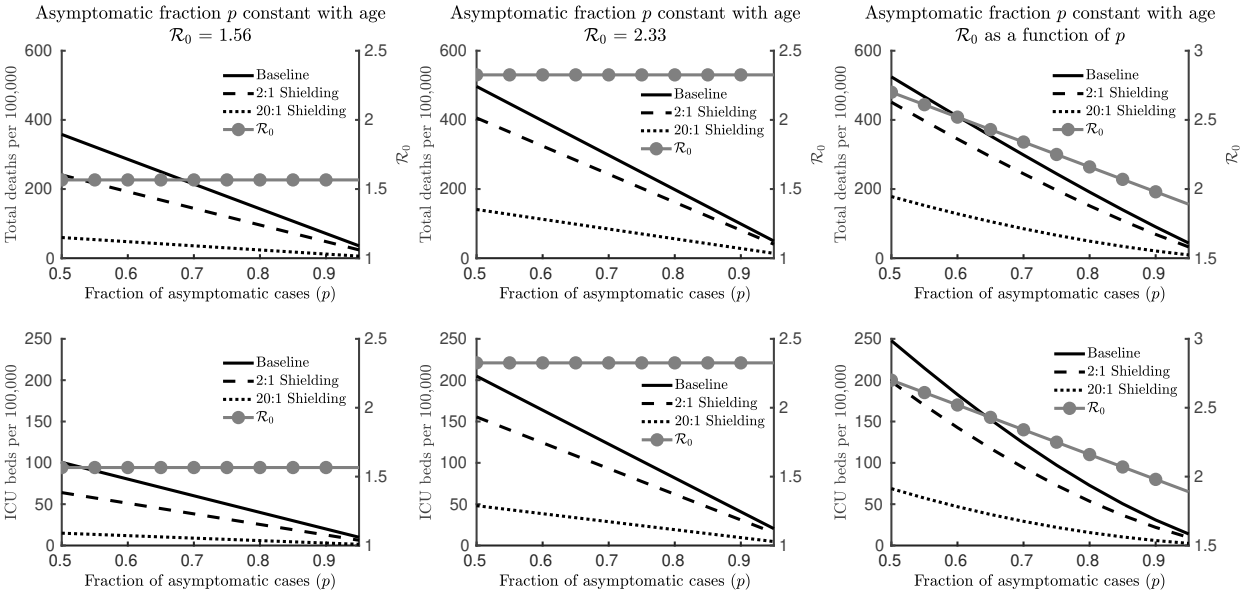

FIG. S4: Impact of p and shielding on the total deaths and the peak ICU cases for a constant R_0 (low scenario left panels, high scenario middle panels) and a dynamic R_0 (right panels). The fraction of asymptomatic p is the same for all ages in the three panels. Shielding offers improvement to outcomes, particularly at lower asymptomatic fractions.

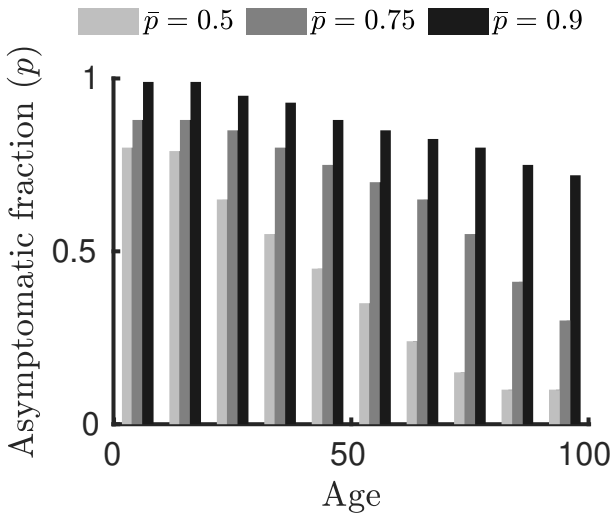

FIG. S5: Age distribution of the asymptomatic fraction p for three different average p: $\bar{p} = 0.5$, $\bar{p} = 0.75$, and $\bar{p} = 0.9$

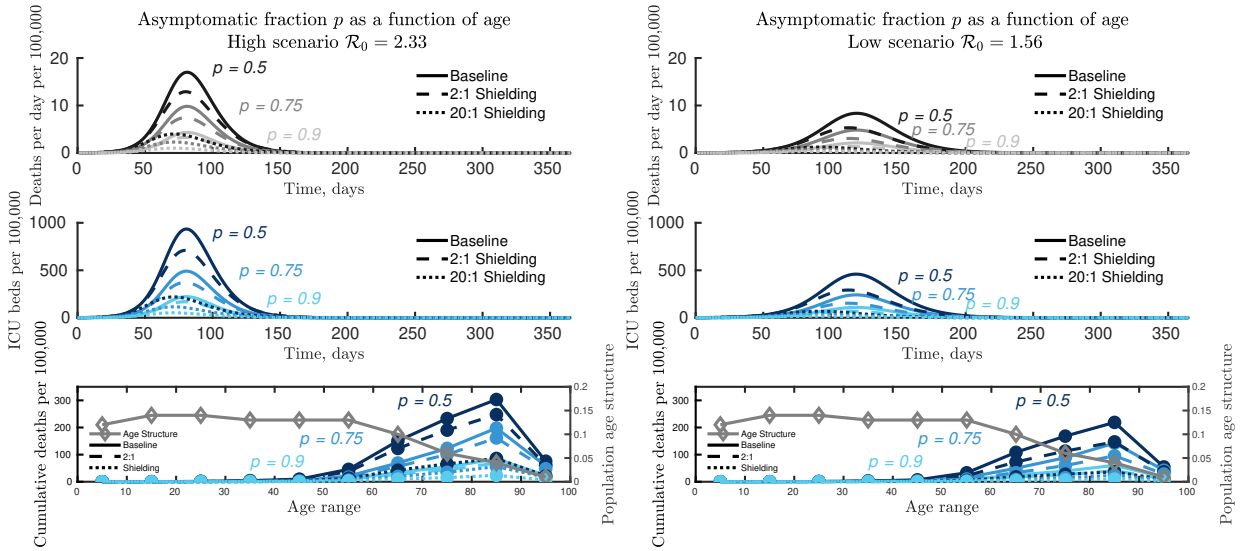

FIG. S6: COVID-19 dynamics in a baseline case without interventions compared to two shielding scenarios ($\alpha = 2$ and $\alpha = 20$) and three age-distributed asymptomatic fraction ($\bar{p} = 0.5$, $\bar{p} = 0.75$ and $\bar{p} = 0.9$) for low scenario ($R_0 = 1.57$ - right panels) and high scenario ($R_0 = 2.33$ - left panels). The impact of immune shielding is robust to observed age-specific variation p, i.e., leading to significant decreases of projected deaths and ICU cases.

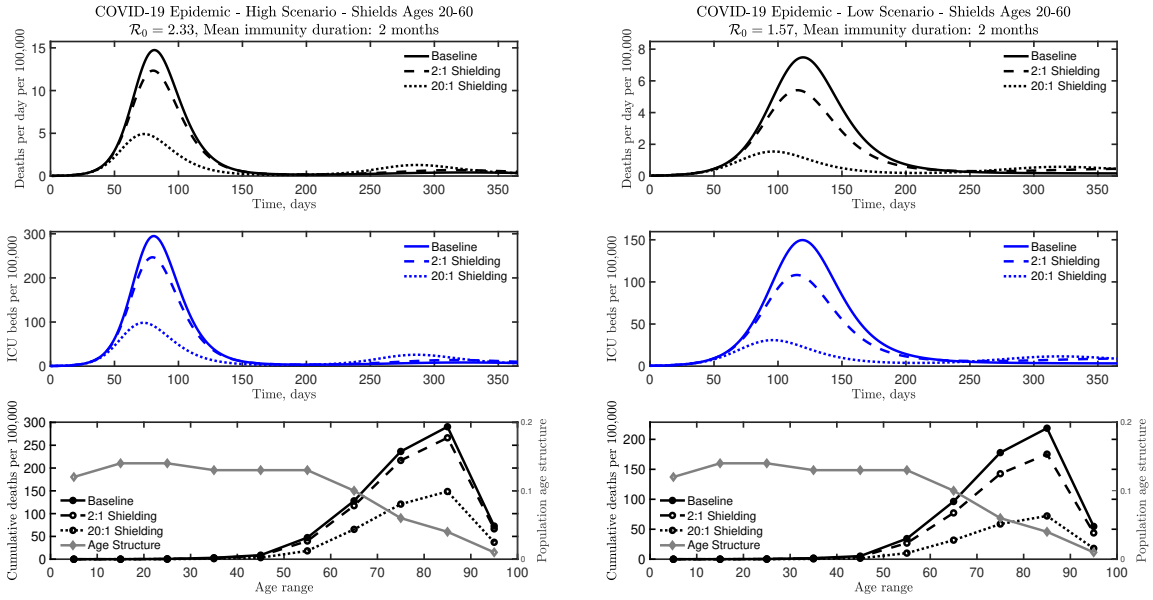

FIG. S7: COVID-19 dynamics for high (left) and low (right) R_0 scenarios. We compared a baseline case without interventions to two shielding scenarios ($\alpha = 2$ and $\alpha = 20$) with a mean immunity duration of 2 months. Immune shielding can still significantly reduce the number of deaths and ICU beds needed for a finite immunity duration.

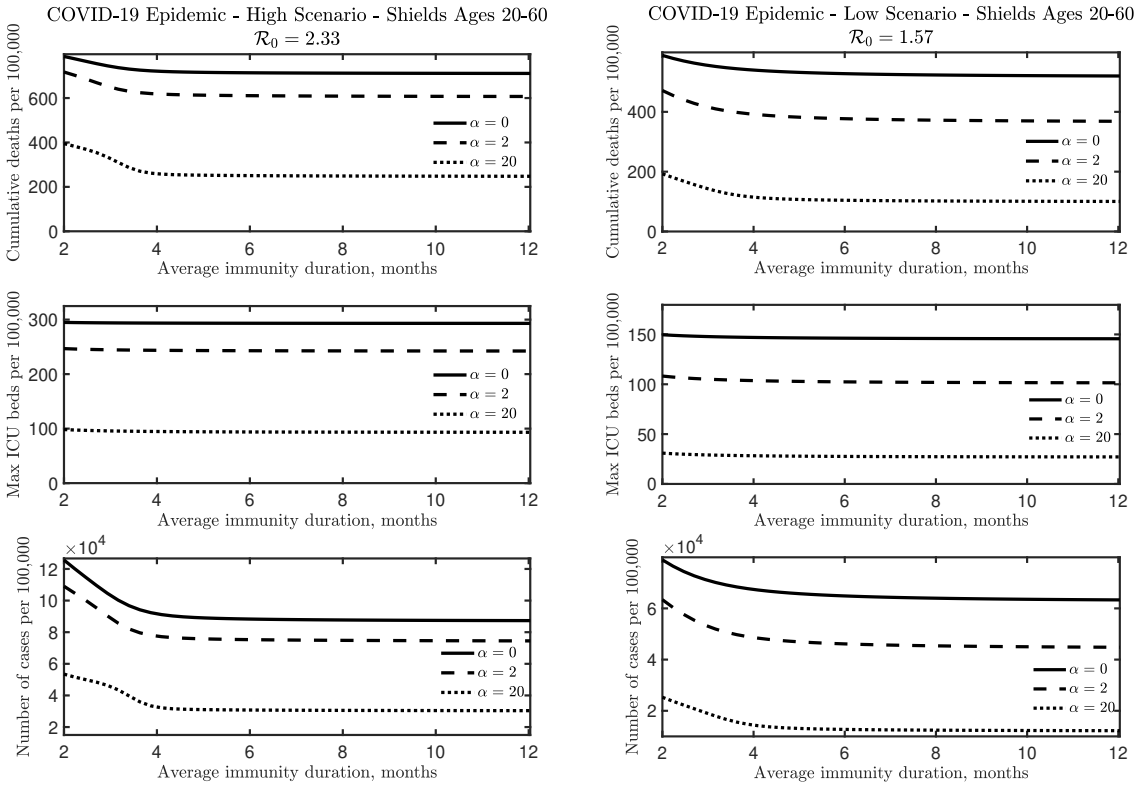

FIG. S8: Comparing the effectiveness of shielding for high (left) and low (right) R_0 scenarios. Shielding is effective at reducing epidemic burden compared to the baseline with no shielding for a wide range of immunity duration. When immunity lasts approximately 4 months or less, re-infection of recovered individuals leads to an increase in the number of deaths and total cases.

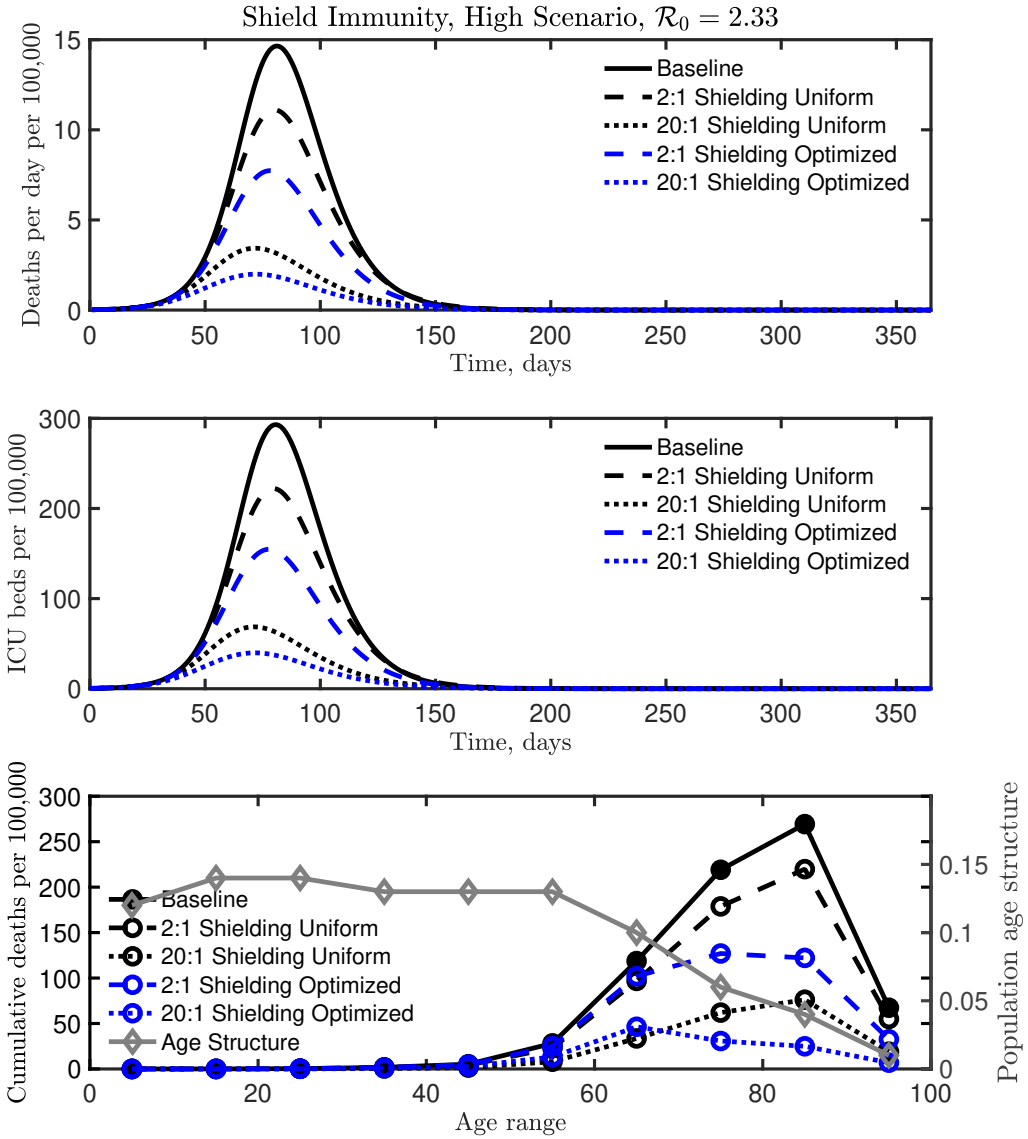

FIG. S9: COVID-19 dynamics in the two shielding scenarios ($\alpha = 2$ and $\alpha = 20$), compared to the scenarios with optimized age dependent shield deployment for the same values of α with the baseline case included for reference. The results are displayed for both high R_0 scenarios. The optimal deployment significantly reduces the total death count and the need for ICU beds for both $\alpha = 2$ and $\alpha = 20$.

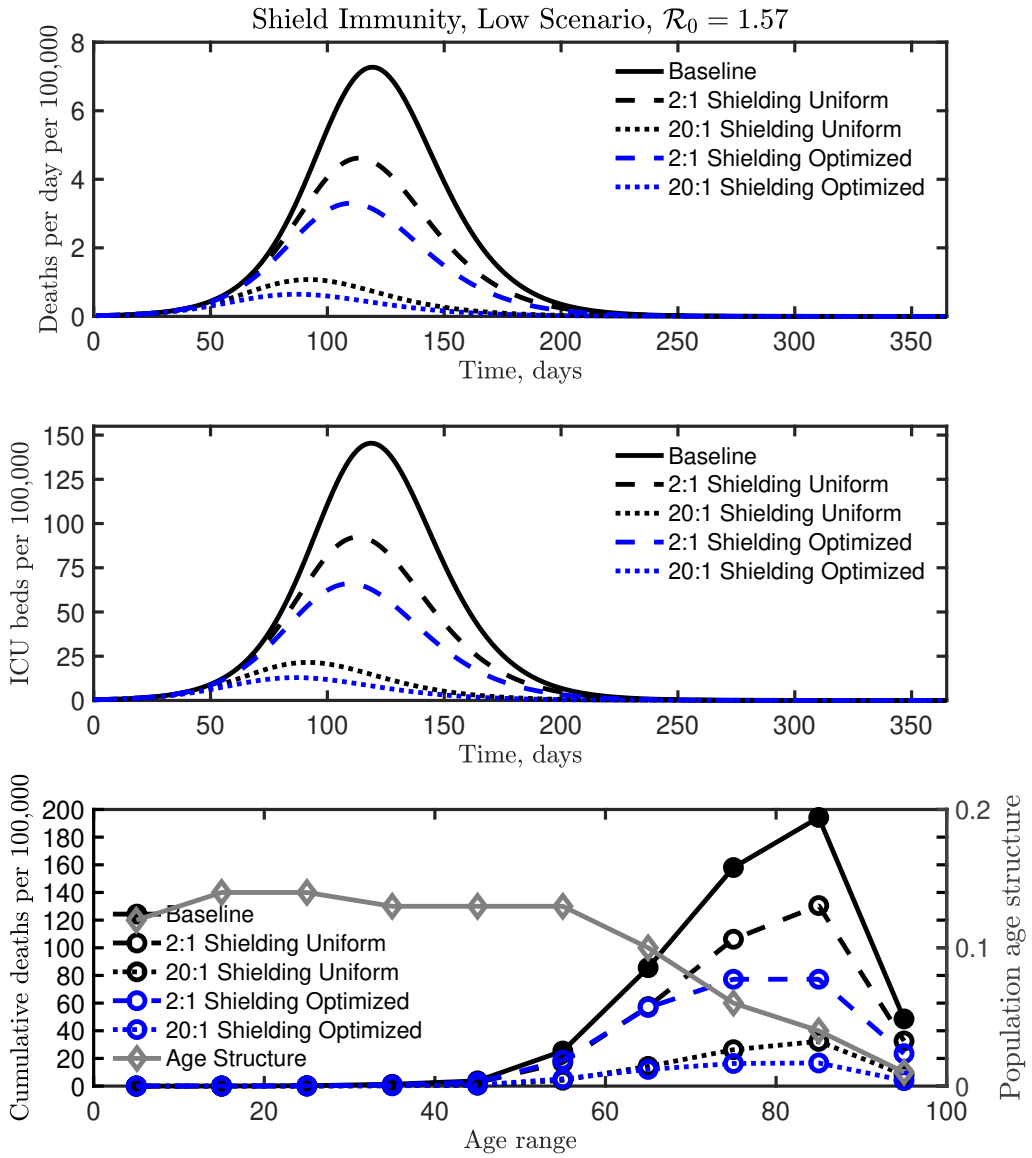

FIG. S10: COVID-19 dynamics in the two shielding scenarios ($\alpha = 2$ and $\alpha = 20$), compared to the scenarios with optimized age dependent shield deployment for the same values of α with the baseline case included for reference. The results are displayed for both low R_0 scenarios. The optimal deployment significantly reduces the total death count and the need for ICU beds for both $\alpha = 2$ and $\alpha = 20$.

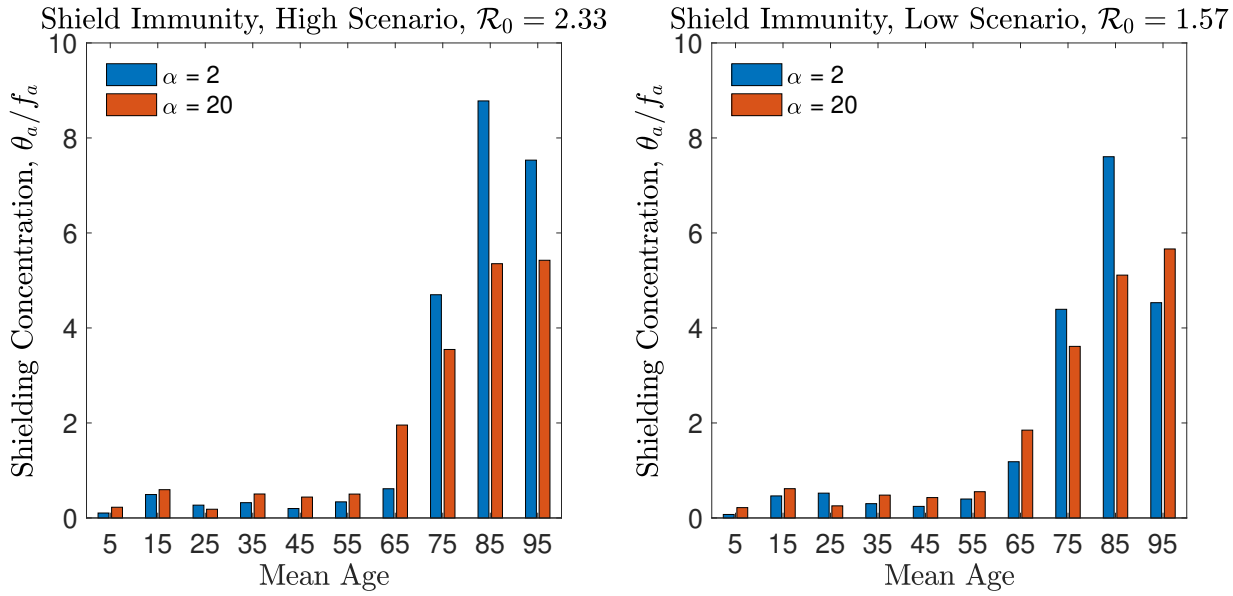

FIG. S11: Optimal shielding concentration for all age classes for the cost defined in (4) for high (left) and low (right) $\mathcal{R}_0$ scenarios. The optimal shielding concentrations (for both scenarios) are obtained via solving optimization problem (eq. 4) with low and high shielding levels. The optimal shielding concentration (θ_a/f_a) is larger for classes with a higher age, which would reduce casualties as the older population is disproportionately affected by COVID-19.

VII. DATA AND SOFTWARE

A. Demography data

Population demographics for US states were obtained from the United States Census Bureau for the year 2018 [5].

B. Figure and simulation codes

All simulation and figure codes used in the creation of this manuscript are available at https://github.com/WeitzGroup/covid_shield_immunity.

1. *MATLAB*

The core model; and extensions to consider variation of asymptomatic to symptomatic cases, the impact of dual intervention of social distancing and serological shielding, the effects of waning immunity, and age-dependent deployment of shields were simulated using MATLAB. Model simulations were numerically integrated using ODE45 [6, 7] in MATLAB R2019a.

2. *Julia*

The core model was reproduced in Julia [8], and extended to look at the affect of different age demographics on disease severity and intervention efficacy. Epidemiological simulations were performed using a 5/4 Runge-Kutta method [9] implemented in the DifferentialEquations.jl package [10].

3. *R*

The core model was reproduced in R. Simulations were performed in R using the ode45 method [6] in the deSolve package [11].

[1] Ferguson N, et al. (2020) Impact of non-pharmaceutical interventions (NPIs) to reduce COVID19 mortality and healthcare demand.

[2] Wu JT, et al. (2020) Estimating clinical severity of COVID-19 from the transmission dynamics in Wuhan, China. *Nature Medicine* pp 1–5.

[3] Whitley D (1994) A genetic algorithm tutorial. *Statistics and computing* 4:65–85.

[4] The MathWorks I (2020) *Global Optimization Toolbox* (Natick, Massachusetts, United State).

[5] Bureau U (2017) Annual estimates of the resident population by single year of age and sex for the United States: April 1, 2010 to July 1, 2017.

[6] Dormand JR, Prince PJ (1980) A family of embedded Runge-Kutta formulae. *Journal of computational and applied mathematics* 6:19–26.

[7] Shampine LF, Reichelt MW (1997) The Matlab ODE suite. *SIAM journal on scientific computing* 18:1–22.

[8] Bezanson J, Edelman A, Karpinski S, Shah VB (2017) Julia: A fresh approach to numerical computing. *SIAM Review* 59:65–98.

[9] Tsitouras C (2011) Runge–Kutta pairs of order 5 (4) satisfying only the first column simplifying assumption. *Computers & Mathematics with Applications* 62:770–775.

[10] Rackauckas C, Nie Q (2017) DifferentialEquations.jl – A Performant and Feature-Rich Ecosystem for Solving Differential Equations in Julia. *Journal of Open Research Software* 5.

[11] Soetaert KE, Petzoldt T, Setzer RW (2010) Solving differential equations in R: package deSolve. *Journal of Statistical Software* 33.